Journal of Building Engineering 12 (2017) 188–195

Contents lists available at ScienceDirect

Journal of Building Engineering

journal homepage: www.elsevier.com/locate/jobe

Thermal insulators with multiple air gaps: Performance, cost and embodied impacts

Luis E. Juanicó[a,*], Alejandro D. González[b]

[a] CONICET and Centro Atómico Bariloche, 8400 Bariloche, Río Negro, Argentina
[b] Instituto Andino-Patagónico de Tecnologías Biológicas y Geoambientales (IPATEC), CONICET and Universidad Nacional del Comahue, 8400 Bariloche, R. Negro, Argentina

ARTICLE INFO

Keywords:
Thermal insulation
Low environmental impact materials
Multilayer insulations

ABSTRACT

The aim of this work is to demonstrate the potential thermal, environmental and cost advantages of a thermal insulation, which consists on several air chambers between layers of an insulation material with low infrared emissivity. The multimodal heat transfer involved (conduction, convection and radiation) is modeled and numerically solved for different materials and designs. The first design proposed uses multiple EPS layers of 1 cm thickness separating air chambers. It achieves global thermal transmittances ranging from 0.439 W/(m^2 K) to 0.126 W/(m^2 K) for 4–13 layers, respectively. In this way, material savings up to 55% were obtained with respect to the solid EPS insulation, leading to lower embodied impacts and cost. A second design, based on thin 0.3 cm MDF panels coated with low-emissivity paint, gave thinner walls than the previous one, but higher embodied impacts and cost. A third design, based on EPS separation layers coated with very low emissivity aluminum foil, leads to significant improvements in all aspects considered. For a given total transmittance of 0.1 W/(m^2 K), this design reaches savings of 77% in material, 66% in cost, 72% in embodied impacts, and 38% reduction in wall width with respect to solid EPS insulations.

1. Introduction

Thermal insulation materials are relevant in environmental assessment of buildings, in stages, construction and operation. In construction, they account on indirect energy and Greenhouse Gas emissions (GHG) embodied in materials when manufactured, transported and installed; and in the operation phase they influence strongly on the energy consumption in heating and refrigeration of buildings. The relative importance of burdens in each stage depends strongly on the thermal quality of building envelopes, being the embodied impacts of greater importance when compared to lower consumption of energy in the operation phase [1].

Higher requirements on low thermal transmittance (*U*) of building envelopes, requires thicker insulations, opening up new questions on environmental footprints embodied in construction materials for thermal efficiency improvements. For instance, a recent innovation on improved Expanded Polystyrene (EPS) consisted in graphite particulates imbedded in the material, giving rise to the new product Graphite Expanded Polystyrene (GPS) [2]. This option is claimed to give a thermal conductivity which is 22% lower than regular EPS. The better transmittance for the same thickness makes the cost of GPS per unit of thermal transmittance similar or slightly lower than that of regular EPS [3]; for instance, a thickness of 80 mm of GPS gives the same thermal transmittance as 100 mm of EPS with the same retailing cost. This improvement also leads to an estimated 30% reduction in manufacturing and transportation burdens [2].

Other efforts are currently directed to achieve thinner materials based on vacuum panels [4], with promising results in experimental stages but still need to find ways of implementation in constructions and lower costs. The vacuum in the panels is clearly an excellent insulator; however, concerns on reliability over time and edge and joints effects affecting thermal conductivity when attaching the panels to the wall have been recently investigated [5,6]. The casing materials have to be vacuum proof and resistant to wearing, thus materials with high conductivity, like aluminum, are used. For instance, a typical equivalent conductivity of fumed-silica vacuum panels is 0.0045 W/(m K) at the center, but the conductivity at the edges due to the enclosing materials can be as much as 0.020 W/(m K), which can be decrease to around 0.015 W/(m K) if taping is performed to avoid convection phenomena at the panels' joints [5]. Lorenzati [6] reported that edge and joint effects could raise the equivalent conductivity of a panel size of 500 × 500 mm to 0.008 W/(m K), which, for a typical 20 mm thick

* Corresponding author.
E-mail addresses: juanico@cab.cnea.gov.ar (L.E. Juanicó), gonzalezad@comahue-conicet.gob.ar (A.D. González).

http://dx.doi.org/10.1016/j.jobe.2017.06.005
Received 20 February 2017; Received in revised form 9 May 2017; Accepted 4 June 2017
Available online 09 June 2017

panel would led to a thermal transmittance of 0.4 W/(m^2 K). In addition, the environmental burdens of carbon emissions and energy used to manufacture vacuum panels with the present technologies are quite high. Karami [7] reported a manufacturing carbon emission for a vacuum panel of 42 kgCO_2eq per m^2, while the corresponding emissions to obtain an equivalent insulation of 100 mm of EPS are around 14 kgCO_2eq per m^2.

On the other hand, the challenge of more sustainable insulating materials from renewable resources of lower environmental impacts led to extensive research in various natural fibers. For instance, Korjenic et al. [8] investigated insulation panels made of flax, jute and hemp with bindings, obtaining thermal conductivities around 0.045 W/(m K). Zhou [9] developed insulation boards with cotton stalk fibers without bindings, in all cases with good performance in both conductivity (0.055 W/(m K)) and low environmental burdens as the basic material is provided by a recycling of residues of crop production. Cereal straw is also a natural fiber much used and with very low conductivity when kept in dry conditions [10], with thermal conductivities around 0.045 W/(m K) [9]. The energy and carbon footprints of insulators based on cereal straw have been studied and compared to conventional EPS. For the same thermal transmittance, straw bale walls can be obtained with only 7 MJ/m^2 against 256 MJ/m^2 of OSB boards and EPS, while building straw and clay blocks on site demand a total energy of 40 MJ/m^2 (see Table 21.1, [11]). Walls and insulations made of agricultural residues also result in much less GHG emissions in the whole manufacturing process, including cultivation burdens. Besides clear environmental advantages and low embodied burdens, the main disadvantages of insulation materials made from natural fibers are high water absorption and poor response to fire. Though, both disadvantages can be dealt with by a careful design of sealing which repeals moisture and would also be fire resistant [12].

In all cases, non-vacuum thermal insulations take advantage of air's low thermal conductivity, and a good thermal insulator should also limit convection phenomena. However, infrared radiation could still account for relevant heat transfers. In the improved EPS case mentioned above, graphite interferes with infrared radiation, increasing total insulation capacity. In a previous work, Saber et al. [13] investigated the use of an air gap incorporating low emissivity surfaces to reduce infrared transmission. The insulation was tested in a basement wall, having one air gap and the EPS surface covered with a foil which emissivity was 0.05. The comparison with a reference wall resulted in an energy saving of 17% for the case of one air space and the foil.

An arrangement of two air-gap cavities with a reflective insulator separating them was investigated by Alev et al. [14], who compared the performance with rock wool in interior insulation of a log-wood wall. These authors found that two air gaps of 25 mm separated by 10 mm reflective insulation gave similar thermal transmittance as 66 mm of rock wool.

In the present work, we have studied the use of a succession of multiple air gaps, separated by surfaces with low emissivity. Among various ways to achieve the insulation array of several air gaps, we have studied three options: 1) EPSW, an array of several air gaps separated by regular white EPS layers; 2) MDFP, an array of several air gaps separated by thin layers of medium density fiberboard (MDF) treated with a low emissivity coating; and 3) EPSF similar to the first option but covering one face of the EPS layer with an Aluminum foil of low emissivity. The performance and costs were compared among each other and to conventional insulation materials, both in thermal transmittance and in embodied energy and greenhouse gas (GHG) emissions. The optimal gap thickness is also discussed, as the insulation capability of each air gap is increased as the number of gaps increases.

2. Materials and methods

2.1. Description of the material proposed

The concept is to build many air chambers separated by thin flat layers of an insulation material with low infrared emissivity. In this way, we obtain a composed material that improves its thermal insulation in relation to the amount of material used, similarly to the case of a double-glass window. However, in contrast with a window, in a wall it is possible to use a larger number of air gaps. As we shall see in the next sections, by enlarging the number of air gaps we obtain three benefits:

1. Every air gap creates insulation, related to their free-convection and conduction mechanisms involved.
2. The infrared radiation through two parallel plates is lower than the radiation emitted by one isolated plate, due to multiple reflections among each other.
3. The temperature difference across each air chamber is reduced by increasing the number of insulation layers. Hence, the optimal air-gap distance is increased and accordingly, the thermal resistance is increased too.

The first study case consists on an assembly of five sheets of 1 cm-thickness EPS separated by five 2.1 cm thickness air cavities, as schemed in Fig. 1. This isolation panel can be realized in external walls of buildings by placing 2.1 cm-width spacers between two contiguous EPS sheets. Therefore, the proposed assembly results in a 15 cm-thickness panel. Detail engineering is out of scope of this work, but anyway this panel could be fixed onto walls in several manners, such as by using through-pass screws attached to the wall [15]. In any case, it can be assume here that the various techniques to fix conventional insulations can be used for the air-gap panels.

2.2. Heat transfer modeling on multiple insulator layers and air cavities

The insulation effect originated by an air cavity is well known, used for example in double-glass windows. The thickness (t_{gap}) of the gap should be optimized in order to minimize the heat transferred by two opposite mechanisms (conduction and convection) through the air gap. The conduction flux q''_{cond} is reduced by increasing the gap thickness, given by

$$q''_{cond} = \lambda_{air}\frac{\Delta T_{gap}}{t_{gap}} = \lambda_{EPS}\frac{\Delta T_{EPS}}{t_{EPS}} = q''_{EPS} \quad (1)$$

where ΔT_{gap} is the temperature difference in front sides of EPS layers

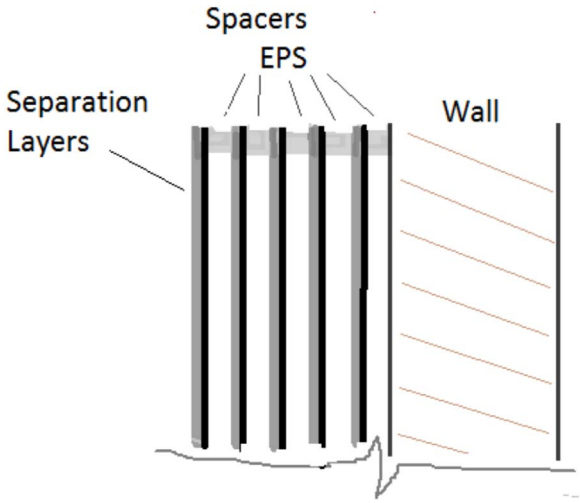

Fig. 1. Schematic drawing of the multilayer insulation panel.

and where λ_{air} is the thermal conductivity of air; the same is valid for a EPS layer. On the contrary, the convection flux q''_{conv} is increased by increasing the gap thickness, since convective cells are promoted by the difference in temperature. This trend is determined by means of Eqs. (2)–(4):

$$q''_{conv} = h\Delta T_{gap} \tag{2}$$

where h is the convection coefficient. For a vertical air cavity of height H assembled between two isothermal plates (T_1, T_2), the convection coefficient h can be calculated from the Nusselt's number (being $Nu = h\, t_{gap}/\lambda_{air}$) by using the well-known engineering correlation [15]:

$$Nu = 0.42 Ra^{1/4} Pr^{0.012} \left(\frac{H}{t_{gap}}\right)^{-0.3} \tag{3}$$

where Pr is the dimensionless Prandtl number of air calculated at the mean temperature $(T_1 + T_2)/2$. Note that the factor $(H/t_{gap})^{-0.3}$ takes into account the effect of convective cells on the convection mechanisms and decreases the Nusselt's number for slender geometries. Even though Eq. (3) is valid for (H/t_{gap}) ratios between 10 and 40, for geometries with H/t_{gap} greater than 40 as are considered here, we assume the maximum reduction achievable by setting $H/t_{gap} = 40$. For this factor greater than 40 is reasonable to assume that the effect caused by convective cells would be smaller or equal to the minimum given by $H/t_{gap} = 40$. This situation is also found, for instance, in double glazing windows, in which the air gap is around 10 mm and thus, H/t_{gap} is usually greater than 40.

The Rayleigh number is defined by:

$$Ra = \frac{g\beta(T_1 - T_2)t_{gap}^3 Pr}{\nu^2} \tag{4}$$

where $g = 9.81\ m/s^2$, and $\beta = 1/T$ [K] is the compressibility module and ν is the kinematic viscosity of air, both considered at the mean temperature in the air gap.

The optimal gap occurs when the dimensionless Nusselt's number (Nu) is equal to the unity, for which the thermal resistance of convection ($R_{conv} = 1/h$) is equivalent to the thermal resistance of conduction ($R_{cond} = t_{gap}/\lambda_{air}$) [16], which means that the convection heat transfer is negligible. For instance, for one air gap having an average difference of 21 °C, the optimal gap is 1.2 cm as it is common in double-glass windows. However, in a multilayer system the temperature difference across each layer, ΔT_{gap}, is lower and so, according to Eq. (4) the optimal air gap is expected to be larger. This enlargement causes noticeably lower heat conduction, as we shall see in next section.

Conduction and convection mechanisms are both present and closely related in air chambers, being the relevance of one mechanism over the other depending mainly on the temperature difference and the gap thickness. There are two ways for calculating the actual heat flux due to both mechanism, according to the value of the Nusselt number (Eq. (3)). If the Nusselt is lower or equal to one, the relevant mechanism is conduction, and convection is negligible. On the contrary, for Nusselt numbers greater than one, the convection mechanism is relevant and the convection correlation includes the conduction effect. For the cases studied here, optimal gaps were chosen to have Nusselt numbers equal to one, and thus both ways of calculating heat flux lead to equal results. For the entire manuscript, we have labeled this flux as conduction-convection, which includes both effects.

On the other hand, and simultaneously with this conduction-convection mechanism, another heat transfer mechanism related to air cavities is the thermal radiation (see Fig. 2) between both EPS sheets that are kept to different temperatures (T_1, T_2). Being known the infrared emissivity of each surface involved $(\varepsilon_1, \varepsilon_2)$, the heat flux transferred by infrared thermal radiation can be estimated by using the well-known model of gray body, in which an effective emissivity (ε_{ef}) must be considered, according to Eqs. (5) and (6) [16,17], where σ (= $5.67 \times 10^{-8}\ W/(m^2 K^4)$) is the Stefan-Boltzmann's constant.

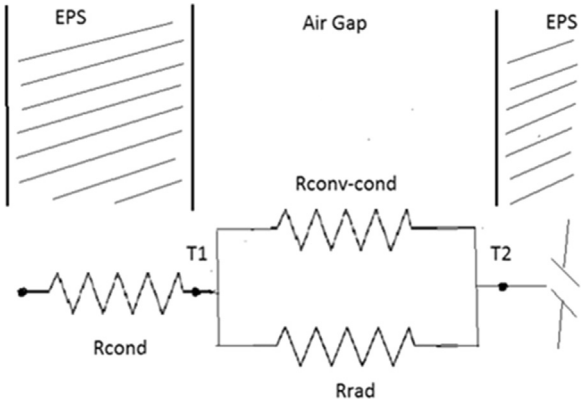

Fig. 2. Schematic drawing of one-dimensional thermal resistances.

$$\varepsilon_{ef} = \frac{1}{\frac{1}{\varepsilon_1} + \frac{1}{\varepsilon_2} - 1} \tag{5}$$

$$q''_{rad} = \varepsilon_{ef}\sigma(T_1^4 - T_2^4) \tag{6}$$

Finally, by using energy conservation, the heat flux through an insulation EPS layer (q''_{EPS}) must be equal to the heat flux transferred by both mechanisms through the neighboring cavity (q''_{gap}) as:

$$q''_{EPS} = q''_{gap} = q''_{cond-conv} + q''_{rad} \tag{7}$$

For the system illustrates in Fig. 1 we consider two boundary conditions: the external outside temperature (T_e), and the temperature of the first insulation layer (T_i) contiguous to the wall. Thus, a nonlinear system of nine equations (similar to Eq. (7)) is obtained (equaling the heat flux through each insulation layer to the consecutive cavity, and conversely, this last to the next layer) having nine variables $(T_1, T_2, \ldots T_9)$, being all these temperatures on internal sides of EPS layers. It is not possible to analytically solve this system due to nonlinear radiation terms, and so it shall be solved numerically.

2.3. Numerical resolution

Firstly, let us fix the values of all thermo-physical properties of air: Pr, β, ν, λ, that are calculated at the mean temperature $(T_m = (T_i + T_e)/2)$ and atmospheric pressure. Under this reasonable assumption (leading to variations down 5%), this one-dimensional thermal problem having nine different regions becomes more symmetric, and so the temperature difference in every insulation layer is the same, and this also occurs in all air cavities. Therefore, the previous system is reduced to only these two temperature differences (ΔT_{EPS}, ΔT_{gap}), which can be related by boundary conditions, as:

$$T_i - T_e = N\,(\Delta T_{EPS} + \Delta T_{gap}) \tag{8}$$

where N is the number of insulation layers, and cavities too. Hence, both temperature differences can be related by using a single (namely x) variable and so, we have to solve numerically the equation of energy conservation, as:

$$q''_{EPS}(x) = q''_{gap}(x) \tag{9}$$

By using an iterative method to solve numerically the last equation, we start with a seed value being $\Delta T_{EPS} = \Delta T_{gap} = \Delta T$, and therefore from Eq. (8) it is easily calculated as: $\Delta T = (T_i - T_e)/2N$. In this way, being known ΔT in one layer, all heat fluxes can be calculated going through Eqs. (1)–(6), and then iterated on ΔT until the balance of energy (Eq. (9)) is verified.

2.4. Energy and carbon embodied in air-gap insulators

Manufacturing construction materials leads to energy use and GHG

Table 1
Energy and GHG emissions for manufacturing 1 kg of EPS.

	Energy (MJ/kg EPS)	GEI ($kgCO_2eq./kg$ EPS)
EPS [18]	145	9.3
EPS [19]	80.8	3.5
EPS [20]	117	17
EPS [21]	142	6.2
EPS [22]	85	6.3
Average of all values	114	8.5

emissions, which are relevant indicators of environmental performance. In this work, we focused on energy use and GHG emissions in manufacturing and transport of materials to the construction site. To assess manufacturing burdens of EPS, MDF and Al-foil we use data from previous works by various authors. For EPS, we use estimations from Harvey for manufacturing EPS in the UK [18], from Anastaselos [19] in Greece, from Bribián [20] in Spain, from Pargana [21] in Portugal, and from Su [22] in China. Table 1 summarizes the results reported by these authors.

The results depicted in Table 1 vary according to different electricity production in each country, use of different fuels for heating, and boundary conditions assumed in each case. As a general case, we will assume that the average of the values given in Table 1 is a fair approach to the energy and GHGs footprint in the production of EPS.

EPS is a lightweight material and therefore transportation can be a significant addition in energy and GHGs when reach the construction site. In order to obtain the impacts we need to set a distance from the factory to the construction site, assumed here as 500 km transported in a 40-ton truck with a fuel efficiency of 0.49 l of diesel per km. The lorry of 14 m long, 2.5 m wide and 2.5 m height is assumed to be fully loaded. Therefore, in 500 km, the transport adds a burden of 7.5 MJ/kgEPS and 0.56 $kgCO_2e$/kg EPS delivered. For every multilayer design, spacers of EPS all around the borders were included, with a thickness of 1 cm and a width according to the air gap distance.

Available data of energy and GHG emissions for the manufacturing of medium density fiberboard (MDF) were obtained by the average reported by Puettmann [23] for the US and Murphy [24]. The average density of MDF considered was 740 kg/m^3, with an embodied energy of 25.4 MJ/kgMDF, and GHGs of 0.99 $kgCO_2e$/kgMDF. It is also assumed that this material is delivered to 500 km, adding 0.33 MJ/kgMDF, and 0.025 $kgCO_2e$/kgMDF. The burdens per kg transported are much lower for MDF than for EPS due to the relative difference in densities.

Data for Aluminum foil were obtained from the European Aluminum Association [25]. The energy and GHG emissions embodied in one kg of Al-foil are 178 MJ and 9.85 $kgCO_2eq$, respectively. We assume the use of an Al-foil of 16 μm thickness [26] and a density of 2700 kg/m^3. The corresponding associated burdens per unit of surface of Al-foil results in 7.7 MJ/m^2 and 0.42 $kgCO_2eq/m^2$, respectively. For simplicity, and assuming them negligible relative to the main materials, the impacts of gluing agents and paints have not been considered.

3. Results

3.1. Analysis of the EPSW multilayer design

First we deal with the case of air gaps separated by EPS, and considering $N = 5$. Table 2 shows input data: physical properties of air and EPS, temperature boundary conditions and geometrical characteristics (N, t_{EPS} and t_{gap}). The emissivity of 0.6 [27,28] and the thermal conductivity of 0.036 are for white EPS with a density of 20 kg/m^3 [3]. Let us remark the unique characteristic of white EPS, having a relatively low infrared emissivity (0.6) compared to other common insulation materials (0.9), which leads to noticeably lower infrared heat radiation, as we shall see next. The performance of this array is depicted in

Table 2
Input data for multilayer with EPSW.

Regular EPS (20 kg/m^3)			
Infrared emissivity	0.6		#
Thermal conductivity	0.036		W/(m K)
Air (cavity)			
Thermal conductivity	0.024		W/(m K)
Thermal diffusivity	$1.40\ 10^{-5}$		m^2/s
Prandtl number	0.7344		#
Geometrical data			
Number EPS and air layers (N)		5	#
EPS thickness (t_{EPS})		1	cm
Gap thickness (t_{gap})		2.1	cm
Temperature boundary conditions			
Internal temperature (T_i)		294	K
External temperature (T_e)		273	K

Table 3
Performance for multilayer $N = 5$ with EPSW.

ΔT_{EPS}	2.02	K
ΔT_{gap}	2.18	K
Nusselt	1.0	#
$q''_{cond\text{-}conv}$	2.44	W/m^2
q''_{rad}	4.88	W/m^2
$q''_{gap} = q''_{EPS}$	7.28	W/m^2
U	0.347	$W/(m^2\ K)$

Table 3. An insulation quality of $U = 0.343\ W/(m^2\ K)$ was obtained, which is similar to the one given by using 10-cm thickness of solid EPS, which would involve double amount of material than the multiple air-gap solution proposed here. The total heat flux q''_{gap} in the air gap is the sum of convection-conduction contribution ($q''_{cond\text{-}conv}$) plus the infrared radiation q''_{rad}. Due to energy balance, the heat flux through the EPS layer equals the total heat flux through the air gap (Eq. (9)). In Table 3, it is relevant to observe that the heat transferred by conduction-convection in the air gap is almost half the transferred by infrared radiation, meaning that the relatively low emissivity of EPS (0.6) is not low enough to minimize radiation effects. In the next sections, we shall investigate other designs having coatings with lower emissivity.

The distance of 2.1 cm for the air gap was optimized by a sensitivity analysis, obtaining the air gap distance that results in a Nusselt number (Nu) equal to one. In this condition, the convection contribution is negligible and the heat is only transferred by conduction through the air gap. Meanwhile, if the distance is increased beyond this optimal, the convection mechanism increases considerably annulling the reduction obtained in the conduction mechanism. Therefore, gap distances close to the optimal should be always used; however, since the optimal gap distance is strongly related to the number of insulation layers, it is necessary to calculate the optimal gap for each case studied.

Let us see how the number of air gaps can improve the insulation quality of the design. Table 4 depicts the results for the EPSW design

Table 4
Sensitivity analysis on the number N of air gaps for the EPSW design.

N	t_{gap} (cm)	Total width (cm)	U (W/ (m^2 K))	$q''_{cond\text{-}conv}$ (W/m^2)	$q''_{rad}/q''_{cond\text{-}conv}$ (#)	$t_{EPS\ equiv}$ (cm)
4	2.0	12.0	0.439	3.17	1.91	8.2
5	2.1	15.5	0.347	2.40	2.03	10.4
6	2.2	19.2	0.286	1.91	2.15	12.6
7	2.4	23.8	0.241	1.52	2.34	14.9
8	2.5	28.0	0.210	1.27	2.46	17.4
9	2.6	32.4	0.185	1.09	2.57	19.5
11	2.75	41.2	0.150	0.84	2.75	24.0
13	2.9	50.7	0.126	0.67	2.93	28.6

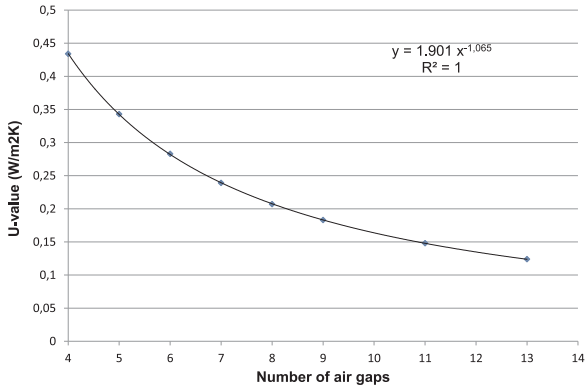

Fig. 3. Thermal transmittance (U value) as a function of the number of layers N for EPSW.

with the number of air gaps between 4 and 13 for which the optimal air-gap distance varies between 2 cm and 2.9 cm, respectively. In this way, the heat transferred by the conduction-convection mechanism through each air chamber is reduced significantly due to both, the air-gap distance increasing and the lower ΔT_{gap} obtained. As the air-gap distance does not affect the radiation term, the ratio $q''_{rad}/q''_{cond\text{-}conv}$ increases. Hence, the U value decreases significantly as the number of layers increases. The last column in Table 4 shows the equivalent solid EPS thickness that should be used in order to obtain the same U value as the design proposed. A significant reduction in material used is obtained; which reaches savings between 51% and 54% in EPS. However, this advantage carries at the same time a larger width of the whole array, as depicted in the third column of Table 4.

Fig. 3 shows the U value as a function of the number of air gaps for the EPSW design. The results are well fitted by a potential function ($U = 1.9011N^{-1.065}$) with an exponent slightly higher than the unit. The unitary exponent would be related to a fully conduction process, but instead the multimodal process involved here leads to a higher exponent. This behavior is also reflected by the ratio in Table 4 ($q''_{rad}/q''_{cond\text{-}conv}$), which increases as the number of layers increases, ranging from 1.88 to 2.90 for 4–13 air gaps, respectively, meaning that the thermal transmittance across air cavities is dominated by radiation. To improve the EPSW design we will study next two options with lower emissivity.

3.2. Analysis of the MDFP-multilayer design

In the previous analysis of the EPSW design, we have increased the insulation quality of the multilayer system by enhancing the conduction resistance of air cavities and separation layers. Now, let us investigate another manner to improve the insulation by working on the infrared heat transmitted. There are two ways for reducing the infrared radiation without increasing the amount of insulation material used:

a) By using thinner EPS layers. For example by using ten 0.5 cm-thickness layers we would use the same amount of material than on the five 1 cm layers, or
b) By using a different material suitable for providing thin layers, and having a lower infrared emissivity.

Proposal a) is not practical regarding standard EPS thickness available and indeed, a thinner EPS layer should be hard to handle. Proposal b) send us back to the problem of finding choices with fairly low emissivity, as we found for EPSW with $\varepsilon = 0.6$. Generally, insulation materials have infrared emissivity close to the unit, meanwhile low-emissivity materials are good thermal conduction ones. However, and keeping in mind that thermal radiation is essentially a surface phenomenon whereas heat conduction refers to the solid material, we can propose now a relatively fair insulation material but coated with a low-emissivity paint. In order to reduce the amount of material it is interesting to explore possible very thin separation layers. The requirement would be to use materials with good mechanical properties and achieve low environmental impacts. On this approach, we have investigated the MDFP design by using 3 mm-thickness MDF layers coated with aluminum paint of infrared emissivity around 0.4, which is the average of a range given in the literature [29]. The choice of MDF was made due to its low energy footprint per kg (24.8 MJ/kgMDF) and that it is manufactured from recycled fibers and its relative cost is low.

Table 5
Sensitivity analysis for MDFP.

N	t_{gap} (cm)	Total width (cm)	U (W/ (m^2 K))	$q''_{cond\text{-}conv}$ (W/m^2)	$q''_{rad}/q''_{cond\text{-}conv}$ (#)	$t_{EPS\ equiv}$ (cm)
4	1.62	7.7	0.502	3.9	1.70	7.0
5	1.75	10.2	0.390	2.9	1.82	9.0
7	1.95	15.7	0.267	1.85	2.04	13.1
9	2.15	22.0	0.202	1.32	2.21	17.3
11	2.3	28.6	0.162	1.01	2.37	21.6
13	2.4	35.1	0.135	0.81	2.49	25.9

Table 5 depicts the results for the MDFP design with the same number of air gaps as in the previous case of EPSW. However, as expected, the optimal air-gap distances have changed, varying between 1.62 cm and 2.40 cm for 4–13 gaps, respectively. These lower distances in comparison with the previous case relates to the higher temperature difference in the air gap, due to the lower thermal resistance in the MDF layer. The U value also decreases significantly as the number of layers increases, but having slightly greater values than the previous EPSW design. Due to lower infrared radiation of the MDFP design, if the number of layers (N) is very large (and so, the conduction mechanism becomes not relevant) the thermal resistance reaches similar values compared to the EPSW design. This behavior is also shown in Fig. 4, which represents U values for different number of MDF layers, fitted by the curve $U = 2.3465\ N^{-1.115}$. Compared to the previous case, this higher exponent leads to better improvement as much as the number of layers increases, reaching, theoretically, both the same U value for $N = 67$. The total width of the array is relatively smaller in MDFP with respect to EPSW, and Table 5 shows that for $N < 7$ it is also comparable to the thickness of solid EPS with equivalent U-value.

In any case, from this analysis we found that the MDFP design with slightly lower emissivity than the EPSW design, does not improve significantly the thermal performance. Therefore, we shall study next the use of a very-low emissivity coating combined with separation layers of good thermal insulation.

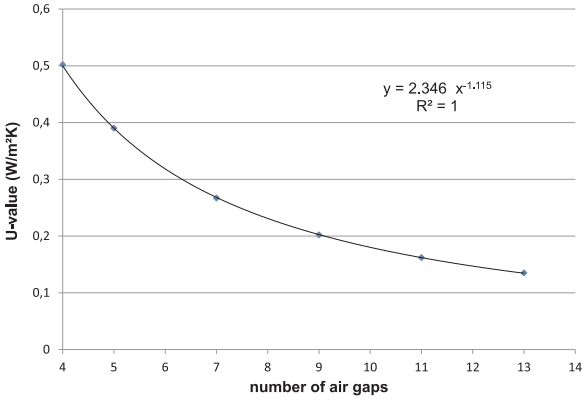

Fig. 4. Thermal transmittance (U value) as a function of the number of layers N for MDFP.

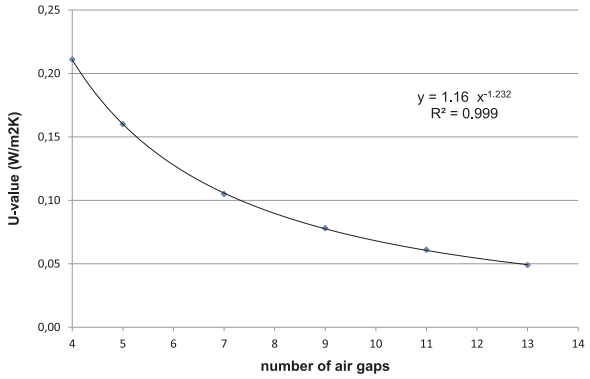

Fig. 5. Thermal transmittance (U value) as a function of the number of layers for EPSF.

3.3. Analysis of the EPSF multilayer design

In this section, we discuss the third proposal, assembled by 1 cm EPS separation layers that are covered on one face with aluminum foil of 16 μm (EPSF design). The aluminum foil adds a surface with very low emissivity ($\varepsilon = 0.04$) [16,27,29]; which reduces significantly the infrared radiation. From Eq. (5), we can observed that the effective emissivity achieved in the air gap is dominated by the aluminum foil term, giving an effective $\varepsilon_{ef} = 0.039$.

Therefore, the heat transmitted by infrared radiation is reduced about seven times with respect to EPSW. Fig. 5 shows the U value as a function of the number of layers (N), which is fitted by a potential function ($U = 1.1631\ N^{-1.232}$) with a slightly higher exponent than previous cases. This trend is explained by the fact that heat conduction through the air gap is the most relevant mechanism in this design, as the thermal conductivity of air is lower than that of EPS. Therefore, larger EPS-material savings were obtained for this case. For instance, Table 6 shows that for N = 5 the multilayer array uses a thickness of 5 cm of EPS, while the equivalent U-value obtained with solid EPS needs 21.6 cm of the material. The savings range from 76% to 82% reductions for 4–13 layers, respectively. In addition, contrary to the previous EPSW and MDFP cases, the total width of the array resulted, for all N, significantly smaller than those needed for the equivalent solid EPS option. Note that, for instance, a very low U-value of 0.1 W/(m^2 K) can be achieved with the use of only 7 cm of EPS and the corresponding foils, in just 21.7 cm of insulation width, instead of 33.3 cm of solid EPS or 28.7 cm of GPS [3].

3.4. Material use, cost, and embodied impacts compared

Let us compare the material used in each design proposed and the equivalent EPS solid that leads to the same U value. Using the previous results, Table 7 summarizes the number of separation layers to obtain transmittance between 0.1 and 0.4 W/(m^2 K). For the cases using EPS, the number of layers also represents the thickness in cm, and thus the savings in material use with respect of using solid EPS were calculated.

Table 6
Sensitivity analysis of N for EPSF design.

N	t_{gap} (cm)	Total width (cm)	U (W/ (m^2 K))	$q''_{cond\text{-}conv}$ (W/m^2)	$q''_{rad}/q''_{cond\text{-}conv}$ (#)	$t_{EPS\ equiv}$ (cm)
4	1.75	11.0	0.211	3.61	0.23	16.6
5	1.95	14.7	0.16	2.69	0.25	21.9
7	2.1	21.7	0.105	1.73	0.28	33.3
9	2.25	29.2	0.078	1.25	0.30	44.9
11	2.4	37.4	0.061	0.96	0.32	57.4
13	2.55	46.1	0.049	0.77	0.35	71.4

Table 7
Number of separation layers (N) used to achieve the same insulation for the three designs studied, and compared to solid EPS insulation (EPSS).

U (W/ (m^2 K))	EPSS (cm)	EPSW (N)	Savings for EPSW (%)	MDFP (N)	EPSF (N)	Savings for EPSF (%)
0.4	8.75	4.32	44.7	4.88	2.38	67.5
0.3	11.6	5.67	45.3	6.32	3.01	70.9
0.2	17.4	8.29	46.6	9.10	4.18	73.1
0.1	34.9	15.9	49.0	16.8	7.34	76.4

Table 8
Comparison of material, embodied energy and GHG, and cost for different insulation designs leading to similar U-value around 0.1 W/(m^2 K).

	EPSS thickness 35 cm	EPSW N = 16	MDFP N = 17	EPSF N = 7
Weight kg/m^2	7.00	3.58	37.8	1.57
Surface Al foil m^2				7.00
weight Al foil kg				0.38
Energy MJ/m^2	850	435	1021	244
GHG kgCO_2/m^2	63.6	32.6	42.1	17.2
Cost USD/m^2	45.6	23.4	42.6	15.5

As explained in Section 2.4, we have also included the EPS spacers in the percentages depicted in Table 7. Savings in use of EPS up to 49% were obtained when EPSW was considered, and up to 76.4% for the Aluminum foil case EPSF.

To compared the embodied energy, GHGs, and the cost of the designs proposed, let us consider an insulation requirement of U = 0.10 W/(m^2 K). This very low value is usually required in envelopes of high efficient housing [30]. Table 8 depicts the results. Designs EPSW and EPSF lead to lower weight per m^2 than solid EPS (EPSS), while MDFP shows much larger weight due to the number of layers needed. The embodied energy and GHGs per m^2 are the lowest for EPSF, even though this design uses Aluminum foil which has high specific embodied impacts. MDFP resulted in the highest embodied energy and EPSS in the highest embodied GHGs, which is related to the reduction in GHG emissions in wood products. The cost per m^2 to achieve 0.10 W/(m^2 K) of insulation was highest for EPSS, followed closely by MDFP [31]. The lowest cost of all the options analyzed resulted for EPSF, which is three times lower than the cost for solid EPS. The design EPSW also has much lower cost than EPSS; however, due to larger total insulation width (64 cm) it may practically not be a better option than EPSS. On the contrary, EPSF has a total width of 21.7 cm, which is significantly smaller than the 35 cm required for the same U value in EPSS. Therefore, we have found that the design using EPS combined with Aluminum foils provides a potential solution to achieve very high efficiency in thermal insulations with much lower embodied impacts and costs. It is interesting to point out that the use a second foil of Aluminum, coating the other face of the EPSF, does not improve the overall performance. This is due to the little effect in reducing the infrared radiation further when it was already much reduced in EPSF. In any case, the double foil would lead to a little better U value but the embodied burdens and the cost would be higher, making the option not convenient with respect to EPSF.

3.5. Discussion

From the various cases studied, we can see that the solutions with lowest thermal emissivity (reflective foils) have the best performance. However, the good performance of air-gap arrays with just white EPS separation layers shows that regular insulations with EPS can be enhanced even for one or two air gaps, at low costs, if air chambers were

considered in the design. In a similar way, the alternative with MDF and paint coatings also led to good results, suggesting the need to review insulation designs including air chambers that may improve the insulation of many wall cover types, without much addition of materials and costs.

A further step to new designs with several layers needs practical developments. For instance, the implementation of wide multiple air-gap arrays to achieve very low thermal transmittance (below 0.1 W/(m^2 K)), may require new technology for the factory manufacturing and the installation on the construction site. However, in all cases that this high level of insulation is reached, it is done with much dedicated structural support and large quantities of materials; therefore the difficulties for implementation are not expected to be larger for multiple air gaps but of a new sort of challenge. In addition, as in all insulations, the arrays of air gaps studied here should be well protected in both exterior and interior applications. It would be easier in exterior applications, and would require a more dedicated moisture barrier in interior insulation [32], considering that the borders can reach large thicknesses. Condensation of moisture in insulations is an important issue. Even though it is out of the scope of the present work, it would need future developments on moisture management in multiple air-gap insulations.

Let us now consider the experimental result reported previously by Alev et al. [14]. These authors compared the performance of two different interior insulations on a log wall, consisting of: 1) 66 mm thickness of mineral wool; 2) two 25 mm air gaps separated by 10 mm reflective mat insulation with very low emissivity coatings ($\varepsilon = 0.08$); and both options covered with a gypsum board. The experiment proved that the claim of the manufacturer of the reflective mat that the assembly results in an insulation equivalent to 200 mm thickness of mineral wool was not verified. In any case, for the purpose of the present work let us notice that options 1) and 2) gave similar experimental thermal transmittances, and can lead to an interesting comparison for the modeling developed above. This model always considers the same number (N) of insulation layers and air chambers. Therefore, in order to apply it to the case of two air gaps with one reflective separator we have reduce the problem to a pair of one air gap and one insulation layer with half the thickness, which can be done due to the linearity of the conduction mechanism inside the insulator.

As seen in previous sections, the calculation depends on the temperature difference, set here to 20 °C in the room side and 7 °C on the exterior side of the air-gap array. The Nusselt number resulted 1.43, the heat flux by conduction-convection was $q''_{cond\text{-}conv} = 4.46$ W/m^2 and the respective radiation flux $q''_{rad} = 1.30$ W/m^2. The total flux was then 5.47 W/m^2, in agreement with the flux reported by Alev et al. (Fig. 6 of Ref. [14]). The resulting thermal transmittance was 0.45 W/(m^2 K) and the equivalent rock wool thickness would be 78 mm. This confirms the findings of Ref. 14 for a temperature difference of 13 K across both insulation options 1) and 2) described above.

4. Conclusions

We have investigated the performance of an insulation system based on multiple air gaps created between flat layers of an insulation material with low infrared emissivity. A model to calculate the multimodal heat transfer by conduction, convection and radiation has been developed, and the numerical method to calculate this kind of systems was performed in a spreadsheet. Three designs have been studied and the obtained total thermal transmittance compared to solid EPS insulation.

A first design, based on air gaps separated by several 1 cm regular EPS was proposed (EPSW). The model allowed calculating the optimum air-gap distance, which varies with the number of layers, and for EPSW ranges from 2.0 cm to 2.9 cm for arrays of 4 and 13 layers, respectively. This effect causes a noticeable reduction of the heat transferred by conduction-convection mechanism, leading to material savings around 50% and similar reductions in cost and embodied impacts. However, as a disadvantage, for EPSW the total width of the insulation wall can be enlarged up to 77%.

Dealing with this drawback, two other designs were studied: the use of thin layers of MDF coated with low emissivity paint (MDFP), and the use of Aluminum foil on EPS separation layers (EPSF). The MDFP design resulted in a reduction of insulation total width, but still having values much larger than solid EPS. For equal heat transmittance, MDFP has lower cost and embodied GHGs than solid EPS; however, the embodied energy is higher.

On the other hand, the EPSF design leads to significant better performance in all aspects considered. For instance, for a given total transmittance of 0.1 W/(m^2 K), this design reaches savings of 77% in material, 66% in cost, 72% in embodied energy and impacts, and 38% reduction in wall width with respect to solid EPS insulations.

The present work makes major contributions in various subjects. First, it provides a practical tool for the thermal analysis of new insulation assemblies based on multiple air-gap chambers and reflective coatings, simplifying the calculation of the important role of convection-conduction and infrared radiation mechanisms in air chambers. Although this concept has been proposed and studied before, the complete thermal modeling developed here allows extending the application of the concept to multiple air chambers. Second, we expect the modeling to help future experimental studies which we are sure will develop after considering the advantages of the multiple gap concept. Third, we were able to assess the environmental embodied energy and GHG emissions of each alternative, and lay out the method to perform the assessment on future insulation proposals within the concept of mixing insulation materials, reflective coatings and air gaps.

Acknowledgements

This work has been supported by the project CONICET PIP 11220130100048CO “Uso eficiente de energía y aprovechamiento del recurso solar en la Patagonia Andina”; and from project Universidad Nacional del Comahue PIN I B191 “Medioambiente y sociedad: peligros naturales y vulnerabilidad en poblaciones de Patagonia Andina”.

References

[1] R. Azari, S. Garshasbi, P. Amini, H. Rashed-Ali, Y. Mohammadi, Energy Build. 126 (2016) 524–534.
[2] Basf, Graphite Polystyrene GPS, 2017. ⟨http://www.neopor.basf.us/performance/⟩.
[3] Retailer a, Expanded Polysterene, Insulation Shop, 2017. ⟨http://www.insulationshop.co/80mm_grey_polystyrene_ewi_graphite.html⟩. (Accessed 11 January 2017).
[4] S. Brunner, K.G. Wakili, T. Stahl, B. Binder, Vacuum insulation panels for building applications: continuous challenges and developments, Energy Build. 85 (2014) 592–596.
[5] B. Choi, T.-H. Song, Investigation of edge taping method applied to vacuum insulation panels, Energy Build. 134 (2017) 52–60.
[6] A. Lorenzati, S. Fantucci, A. Capozzoli, M. Perino, Experimental and numerical investigation of thermal bridging effects of jointed vacuum insulation panels, Energy Build. 111 (2015) 164–175.
[7] P. Karami, N. Al-Ayish, K. Gudmundsson, A comparative study of the environmental impact of Swedish residential buildings with vacuum insulation, Energy Build. 109 (2015) 183–194.
[8] A. Korjenic, V. Petranek, J. Zach, J. Hroudova, Development and performance valuation of natural thermal-insulation materials composed of renewable resources, Energy Build. 43 (2011) 2518–2523.
[9] Xiao-Yan Zhou, Fei Zheng, Hua-guan Li, Cheng-long Lu, An environment-friendly thermal insulation material from cotton stalk fibers, Energy Build. 42 (2010) 1070–1074.
[10] A.D. González, Energy and carbon embodied in straw and clay wall blocks produced locally in the Andean Patagonia, Energy Build. 70 (2014) 15–22.
[11] A.D. González, et al., (Chapter 21) Assessment of the energy and carbon embodied in straw and clay masonry blocks, in: Pacheco Torgal, et al. (Ed.), Eco-efficient Masonry Bricks and Walls: Design, Properties and Durability, 2015, pp. 461–480 http://www.sciencedirect.com/science/article/pii/B9781782423058000218.
[12] E. Latif, M.A. Ciupala, S. Tucker, D.C. Wijeyesekera, D.J. Newport, Hygrothermal performance of wood-hemp insulation in timber frame wall panels with and without a vapour barrier, Build. Environ. 92 (2015) 122–134.
[13] H.H. Saber, W. Maref, M.B. Swinton, Thermal response of basement wall systems with low-emissivity material and furred airspace, J. Build. Phys. 35 (4) (2011)

353–371.
[14] Ü. Alev, T. Kalamees, E. Arumägi, S. Ilomets, Comparison of thermal performance of mineral wool and reflective insulation on internally insulated log wall, in: Proceedings of Healthy Buildings 2012: Healthy Buildings 2012, Brisbane, Australia, 8–12 July 2012, Brisbane, Queensland University of Technology, Australia, 2012, pp. 1–6.
[15] Screwfix, 2016. ⟨http://www.screwfix.com/p/rawlplug-long-expansion-hammer-in-insulation-fixings-160-x-10mm-250-pack/57658⟩.
[16] F.P.Y. Incropera, D.P. DeWitt, Fundamentals of Heat and Mass Transfer, 7th ed., John Wiley, United States of America, 2011 (ISBN 978-0470-50197-9).
[17] Y.A. Cengel, Heat transfer, A Practical Approach, 2nd ed., Mc-Graw Hill, United States of America, 2003 (ISBN 978-0071-15150-4).
[18] L.D.D. Harvey, Net climatic impact of solid foam insulation produced with halocarbon and non-halocarbon blowing agents, Build. Environ. 42 (8) (2007) 2860–2879.
[19] D. Anastaselos, E. Giama, A. Papadopoulos, An assessment tool for the energy, economic and environmental evaluation of thermal insulation solutions, Energy Build. 41 (11) (2009) 1165–1171.
[20] I.Z. Bribián, A.A. Usón, S. Scarpellini, Life cycle assessment in buildings: state-of-the-art and simplified LCA methodology as a complement for building certification, Build. Environ. 44 (12) (2009) 2510–2520.
[21] N. Pargana, M.D. Pinheiro, J.D. Silvestre, J. de Brito, Comparative environmental life cycle assessment of thermal insulation materials of buildings, Energy Build. 82 (2014) 466–481.
[22] X. Su, et al., Life cycle inventory comparison of different building insulation materials and uncertainty analysis, J. Clean. Prod. 112 (2016) (2016) 275–281.
[23] M. Puettmann, E. Oneil, J. Wilson, Cradle to Gate Life Cycle Assessment of U.S. Medium Density Fiberboard Production, WoodLife Environmental Consultants, CORRIM, and Oregon State University report, 2013. Available at (20 Nov 2016). ⟨http://www.corrim.org/pubs/reports/2013/phase1_updates/MDF%20LCA%20final%20Sept%202013.pdf⟩.
[24] F. Murphy, G. Devlin, K. McDonell, Greenhouse gas and energy based life cycle analysis of products from the Irish wood processing industrial, J. Clean. Prod. 92 (2015) 134–141.
[25] European Aluminium Association, Environmental Profile Report for the European aluminium Industry, 2013. ⟨http://european-aluminium.eu/resource-hub/?id=1876⟩. (accessed 12 January 2017).
[26] Retailer b, Aluminum Foil, 2017. ⟨http://www.staples.com/HFA-BWK-FOIL-FTL-Aluminum-Foil-Roll-12-x-500-/product_1524155⟩ (Accessed 11 January 2017).
[27] Thermography b, Emissivity Table, 2017. ⟨http://www.infrared-thermography.com/training.htm⟩. (Accessed 12 January 2017).
[28] M. D'Orazio, C. Di Perna, E. Di Giuseppe, M. Morodo, Thermal performance of an insulated roof with reflective insulation: field tests under hot climatic conditions, J. Build. Phys. 36 (3) (2012) 229–246.
[29] Thermography a, Emissivity Values for Instrument Calibration, 2017. ⟨http://www.scigiene.com/pdfs/428_InfraredThermometerEmissivitytablesrev.pdf⟩. (Accessed 12 January 2017).
[30] M. Wall, Energy-efficient terrace houses in Sweden: simulations and measurements, Energy Build. 38 (2006) 627–634.
[31] Retailer c, Medium Density Fiberboard, 2017. ⟨http://www.easy.cl/es/easy-chile/construccion/tableros/mdf-y-aglomerados-/tablero-mdf-3x1520x2440-milimetros-desnudo-masisa-488110⟩. (Accessed 11 January 2017).
[32] Ü. Alev, T. Kalamees, Avoiding mould growth in an interiorly insulated log wall, Build. Environ. 105 (2016) 104–115.